Received: 11 February 2023 | Revised: 11 September 2023 | Accepted: 27 September 2023

DOI: 10.1111/ejn.16169

RESEARCH REPORT

EJN European Journal of Neuroscience FENS WILEY

Cognitive-perceptual traits associated with autism and schizotypy influence use of physics during predictive visual tracking

Chloe Cooper[1,2] | **Andrew Isaac Meso**[2,3]

[1]Acute Inpatient Psychology, Dorset Healthcare University NHS Foundation Trust, Poole, UK

[2]Psychology and Interdisciplinary Neuroscience Group, Bournemouth University, Poole, UK

[3]Neuroimaging Department, Institute of Psychiatry, Psychology and Neuroscience, King's College London, London, UK

Correspondence
Andrew Isaac Meso, Neuroimaging Department, Institute of Psychiatry, Psychology and Neuroscience, King's College London, London, UK.
Email: andrew.meso@kcl.ac.uk

Funding information
Bournemouth University; King's College London

Edited by: John Foxe

Abstract

Schizophrenia and autism spectrum disorder (ASD) can disrupt cognition and consequently behaviour. Traits of ASD and the subclinical manifestation of schizophrenia called schizotypy have been studied in healthy populations with overlap found in trait profiles linking ASD social deficits to negative schizotypy and ASD attention to detail to positive schizotypy. Here, we probed the relationship between subtrait profiles, cognition and behaviour, using a predictive tracking task to measure individuals' eye movements under three gravity conditions. A total of 48 healthy participants tracked an on-screen projected ball under familiar gravity, inverted upward acceleration (against gravity) and horizontal gravity control conditions while eye movements were recorded and dynamic performance quantified. Participants completed ASD and schizotypy inventories generating highly correlated scores, $r = 0.73$. All tracked best under the gravity condition, producing anticipatory downward responses from stimulus onset which were delayed under upward inverted gravity. Tracking performance was not associated with overall ASD or schizotypy trait levels. Combining measures using principal components analysis (PCA), we decomposed the inventories into subtraits unveiling interesting patterns. Positive schizotypy was associated with ASD dimensions of rigidity, odd behaviour and face processing, which all linked to anticipatory tracking responses under inverted gravity. In contrast, negative schizotypy was associated with ASD dimensions of social interactions and rigidity and to early stimulus-driven tracking under gravity. There was also substantial nonspecific overlap between ASD and schizotypy dissociated from tracking. Our work links positive-odd traits with anticipatory tracking when physics rules are violated and negative-social traits with exploitation of physics laws of motion.

KEYWORDS
ASD, eye movements, gravity, prediction, schizotypy

Abbreviations: FEF, frontal eye fields; PCA, principal component analysis; RMSE, root mean square (position tracking) error; SATQ, Subthreshold Autism Trait Questionnaire; SPQ, Schizotypal Personality Questionnaire.

1 | INTRODUCTION

Schizophrenia and autism spectrum disorders (ASD) are common heterogeneous conditions that have historically been considered distinct. Recently, cognitive and behavioural overlap between them has been suggested following observations that they share similarities in pathological social and physiological characteristics and behaviours that may be signatures of their underlying comorbidity (Chisholm et al., 2015). Clinically motivated research has focused on establishing practical rigid diagnostic clarification with limited consideration of variation within specific symptoms (Ford et al., 2018). Improving the mechanistic understanding of cognition and behaviour that is typical of these conditions and concurrently probing the underlying genetic and neural correlates will be crucial for better characterisation and could ultimately enhance diagnostic and treatment practices (De Giorgi et al., 2019; Klopper et al., 2017). We study phenotype variability within a healthy population with a behavioural task designed to provide insights into sensorimotor mechanisms likely to be disrupted by common ASD and schizotypy traits.

Schizotypy refers to a set of personality traits mirroring symptoms of schizophrenia at a subclinical level, characterised by dimensions (positive, negative and disorganised) that run on a continuum from healthy to psychosis (Nelson et al., 2013; Raine, 1991). Positive symptoms include odd beliefs, unusual perception and negative affect, while negative symptoms include avolition, asociality and diminished positive affect. The positive and negative dimensions of schizotypy have been psychometrically validated as constructs across cultures and shown to be distinctly linked to schizophrenia and the prodrome stage preceding psychotic symptoms (Barrantes-Vidal et al., 2013). Schizotypy can therefore be considered part of a continuum with clinical pathology the extreme manifestation. One unifying emerging view is that schizophrenia may be the result of disrupted predictive neural mechanisms with heterogeneous symptom profiles explained as disruptions to different underlying neural circuits. It is referred to as the predictive-coding perspective (Sterzer et al., 2019). ASD patients also exhibit heterogeneous symptom profiles including sensory hypersensitivity, difficulties with theory of mind, deficits interacting with moving objects and repetitive behaviours. A growing perspective in ASD research is referred to as the predictive impairment in autism hypothesis. Proponents suggest that there may be a unified explanation for the broad range of deficits observed and the link hinges on individuals' prediction of states of the world, an idea which shows marked similarity with the predicitive-coding perspective for Schizophrenia (Sinha et al., 2014). These converging perspectives in studying the causes of ASD and schizotypy therefore raise the question about the role of predictive processing in understanding overlaps in their behavioural, cognitive and perceptual deficits.

Much recent research has been dedicated to characterising commonalities within self-reported traits. In a large healthy sample ($N = 1678$), Ford et al. (2018) used latent profile analysis to identify eight clusters of trait characteristics encompassing dimensions of schizotypy and ASD. These clustered subgroups included one with psychosocial difficulties which appeared to represent a shared social autism-negative schizotypy domain consistent with previous work (Abu-Akel et al., 2018), another autism-schizotypy subgroup with constituent measures reflecting nonspecific overlap of ASD and schizotypal traits, and notably measures of psychosis and those associated with a moderate aspect of schizotypy appeared to be independent. More recent work further identified consistent overlapping and diametrically opposed facets of phenotypes. With a sample of $N = 640$, Nenadić et al. (2021) used principal components analysis (PCA) to study multiple psychometric measures of schizotypy and ASD in a German and separate Swiss/French population. They identified loss of function and communication deficits as phenotypes of ASD traits showing convergence with negative and disorganised features of schizotypy. However, attention to detail in ASD was diametrically opposed to positive schizotypal trait dimensions.

Both schizophrenia and ASD engender perceptual and cognitive characteristics or endophenotypes that can be measured under experimental lab conditions. Such lab measures can complement self-reported or expert assessed traits with a more objective output. Poor smooth pursuit eye movements (SPEM) are an established endophenotype of schizophrenia and schizotypy. Deficits in motion processing and target prediction in schizophrenia contribute to SPEM abnormalities (Barnes, 2008) with findings replicated in schizotypy (Koychev et al., 2016). Often experimentally isolated and studied as separate systems, in an ecological context, SPEM and saccadic movements form part of a complementary sensorimotor repertoire used to interact with viewed scenes. Dynamic eye movements are served by continuous estimates of future eye positions and velocity-related error signals (Goettker & Gegenfurtner, 2021). Along the pathway driving the oculomotor response, there are dynamic interactions between sensory input, predictions and errors estimated by internal processes enabling tracking while maintaining perceptual stability (Goettker et al., 2019). It has been established in ball catching experiments on astronauts with conditions both in space and on earth that humans can use internalised

knowledge about the physics of gravity to move their hands for just in time well executed catches (McIntyre et al., 2001). In space, without gravity, the ball moves at constant speed, and catching is negatively impacted implying that this predictive model is automated and pre-attentive. We previously took advantage of this internalised predictive system to establish experiments that showed that motion tracking under gravity and by contrast inverted gravity conditions provide a means of studying individual differences in the extent to which participants incorporate predicted gravity into cognitive processing (Meso et al., 2020). Predictions of future positions of projected parabolically moving objects exploit knowledge of gravity and participants' eye movements have been shown to be guided by prediction (Delle Monache et al., 2015) though this is achieved with different levels of performance across participants (Jörges & López-Moliner, 2019). Observers were generally capable of distinguishing different settings of gravitational acceleration of parabolic trajectories with poor precision (Jörges et al., 2018).

ASD has been shown to drive deficits in ocular motor function with a recent review identifying saccade accuracy, inhibitory control and impaired tracking as common issues noted in a range of studies in clinical populations (Johnson et al., 2016). The initiation of eye movements and disengaging from targets did not seem impaired in ASD groups. Of particular interest to us within the review were findings that clinical groups showed more substantial errors in antisaccade tasks than controls, an indication of poorer inhibitory control. In several smooth pursuit experiments reported, clinical groups generally had a poorer gain in tracking velocities (the dynamic ratio of the eye speed over the stimulus speed) with more marked differences between groups during the earlier phase of tracking, called the open-loop, than during the later so-called closed period starting around 200 ms from stimulus onset.

The use of eye movements recorded during dynamic tasks therefore provides an interesting opportunity to elucidate mechanisms disrupted by both schizotypy and ASD. The functioning of the ocular motor system is underpinned by a distributed network of brain areas within cerebral cortex, cerebellum and the brain stem (Masson & Perrinet, 2012). The cerebellum is integral to problem-solving in spatial orientation due to its role in vestibular processing and representations of gravity needed for behaviour rely on it (MacNeilage & Glasauer, 2018). In macaques, the cerebellum has been shown to encode predictive signals which disentangle sensory consequences of gravity from self-movements (Mackrous et al., 2019). Human cerebellar lesion patients exhibited deficits in perception of gravitational direction in a perceived tilt task (Dakin et al., 2018). Activity in the frontal eye fields (FEF), an area that contributes to target prediction with an internal representation, has been found to be reduced during smooth pursuit in schizophrenic patients (Faiola et al., 2020). Corresponding reductions have not been observed in schizotypy (Meyhöfer et al., 2015). Furthermore, using functional Magnetic Resonance Imaging and connectivity analyses, patients with recent-onset psychosis and low-schizotypy controls were indistinguishable based on brain activity during smooth pursuit performance. However, using machine learning, participant group classifications were made using a right FEF seed region, based on its connectivity within subcortical and cortical structures, frontal cortex, cerebellum and hypothalamus (Schröder et al., 2022). As interconnected cortical areas MT (middle temporal) and MST (medial superior temporal) process visual motion signals producing commands for smooth pursuit, FEF may regulate this output with real-time gain control (Churchland & Lisberger, 2002; Ono, 2015). These findings, which highlight a potential predictive role for FEF within a wider network, suggest that individual variation in visual tracking ability is more subtle than previously thought and demands a fine-grained exploration of prediction, representation and information integration mechanisms.

In a recent study, high schizotypy participants had worse performance during predictive pursuit than a control low-schizotypy group, but SPEM in a sinusoidal tracking task showed no differences (Faiola et al., 2020). In the prediction task, participants tracked a stimulus that moved at a constant velocity and was pseudorandomly blanked in half the trials, with instructions given to continue eye movements during the blank. These findings imply that the prediction deficit is separate from general SPEM performance even along a sinusoidal path, consistent with the findings of Meso et al. (2020), who manipulated prediction using two gravity conditions. In the task, participants tracked a simulated projected ball under gravity, and the unfamiliar inverted upward gravity conditions and performance was seen to be worse on average under inverted gravity from trial onset with differences persisting for over 200 ms. This deficit was specific to the vertical gravity direction and not seen in comparisons of the horizontal direction traces. Participants in the tasks had their traits of schizotypy, anxiety and general health measured by self-reported inventories, and only schizotypy trait levels were seen to be associated with tracking performance under inverted gravity condition. In PCA analysis, the inventories that were used in their entirety and not decomposed down into subtraits (e.g. positive and negative schizotypy) dominated the components identified, and no systematic pattern

associated with eye tracking could be characterised. The work of Meso et al. (2020) therefore left some glaring follow-up questions. First, was the effect observed specific to the vertical direction in which gravity is experienced to act or could it be recreated with horizontal ball accelerations? Second, could associations between traits and eye movements be better characterised by decomposing schizotypy into positive, negative and disorganised scores and leaving out the control inventories? Third, because of the element within the task of applying physics-based predictive estimation, could ASD traits show similar results to schizotypy that might reveal commonalities between the conditions? Finally, to what extent does the performance change over the course of the 160 trials within a given block?

The current work is the follow-up to Meso et al.'s (2020) research and will focus on addressing three main questions. First, can we conceptually replicate that previous work on tracking under gravity (Meso et al., 2020) showing the main result of poorer performance under inverted gravity with additional controls for gravity direction? Second, can we unveil differences in tracking performance dynamics and organise them in terms of anticipation (pre-sensory response), early open-loop and later closed-loop responses? Finally, can we characterise the multidimensional relationship between schizotypy and ASD subtraits and link these to eye-tracking measures for a meaningful interpretation of clusters? We take a combined experimental and theoretical approach and answer each one of these questions in turn.

2 | MATERIALS AND METHODS

2.1 | Participants

We tested 48 participants (29 female, 19 male, age $M = 22.1$, SD $= 3.9$, IQR $= \{19,23\}$) recruited by opportunity sampling at Bournemouth University. Participants received £5 for their time. The study was approved by the Research Ethics Committee of Bournemouth University and was carried out in accordance with the principles of the Declaration of Helsinki. Owing to multivariate design complexity, participant numbers could not be determined by standard power calculation using an expected effect size, required power and fixed alpha. Previous research carried out using similar eye-tracking tasks have required 6 to 10 participants to sufficiently test for differences across conditions (e.g. Meso et al., 2016, 2022). Trait inventory participant requirements are typically higher than this so in the current work, inventories will determine N. Previous rough power estimates suggested about 45 participants (Meso et al., 2020), as did a recent reliability and replicability study on SPEM and traits (Schröder et al., 2021).

2.2 | Stimulus and materials

Stimuli were generated on a Windows 7 PC running bespoke Matlab (Mathworks) routines in Psychtoolbox (Brainard & Vision, 1997; Pelli, 1997). Presentation was on a Cambridge Research Systems 32′ Display++ Monitor with 1920 × 1080-pixel resolution and 100 Hz refresh rate. The monitor was placed 80 cm from participants in an ambiently lit quiet laboratory. Eye movements were recorded from the right eye using an SR Eyelink Video eye tracker operating at 1000 Hz with movement restricted by a head/chinrest (See Figure 1a). The stimulus was based on Meso et al. (2020), with sizes scaled to an on-screen virtual square with sides of 900pix containing the stimulus presentation area of 23.4 degrees of visual angle (°). The black ball had 0.21° diameter with motion characterised by Equations (1) to (4).

$$V_x(t) = d \cdot S_x \tag{1}$$

$$P_x(t) = X_0 + d \cdot S_x t \tag{2}$$

V_x in Equation (1) is the constant horizontal component of the speed with S_x set from {4, 16} °/s randomised in each individual trial for fast/slow and direction d set from {−1,1} for left/right randomised in each trial. The time-varying horizontal position P_x in Equation (2) depended on stimulus speed S_x starting at the centre of the screen, X_0 at the initiation of each trial.

$$V_y(t) = S_y + \varepsilon + g \cdot t \tag{3}$$

$$P_y(t) = Y_0 + (S_y + \varepsilon)t + (g \cdot t^2)/2 \tag{4}$$

V_y in Equation (3) is the vertical speed component initiated as $S_y = \pm 2°/s$ and ε is a randomised real number drawn on each trial from a flat continuous distribution of ± {0 to 0.5}°/s away from the direction of acceleration g, which is $\pm 9.81°/s^2$ for the gravity (+) and the direction against gravity (−) conditions. The position P_y in Equation (4) incorporates the initial position at the centre of the screen Y_0 and the integration of Equation (3) for position with respect to time. At the given viewing distance, the resulting motion dynamics is that expected for a ball just smaller than a professional soccer ball.

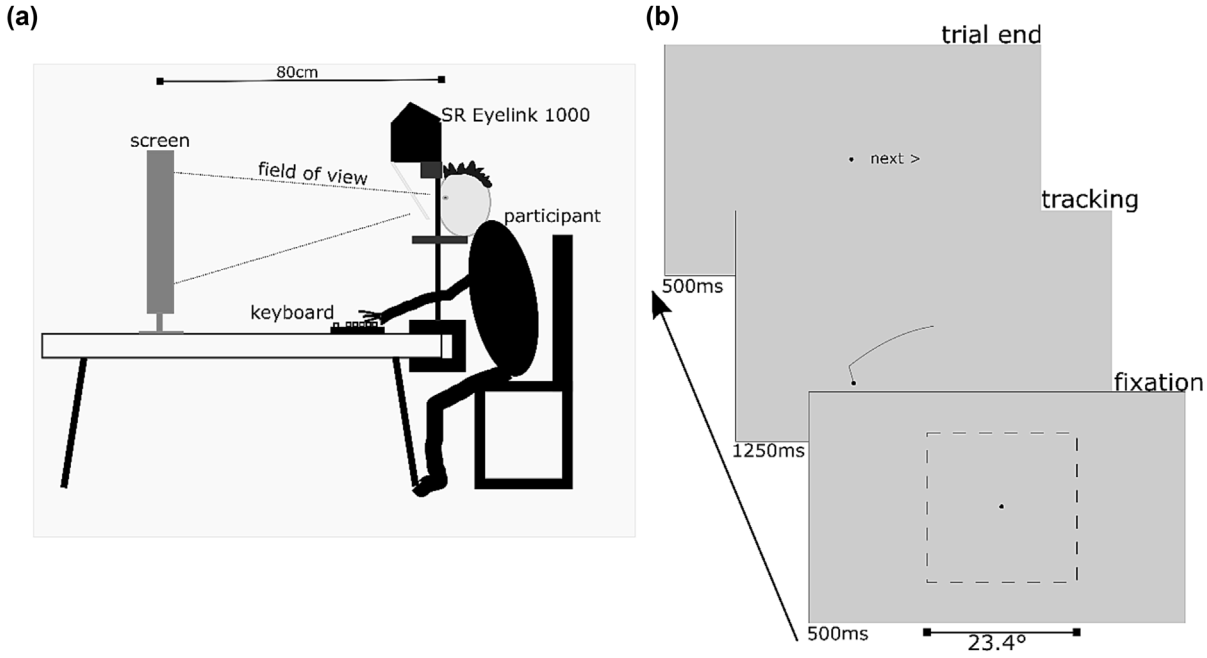

FIGURE 1 Task and set up illustration. (a) An illustration of a participant in the set up with the tower mounted SR 1000 Eyelink video eye tracker, 32′ display++ screen and viewing position. (b) Three phases of the task with a 500 ms fixation also showing the virtual stimulus coverage square area which acted as unseen barriers/walls to the ball shown in square in dashed lines (to guide the reader: not shown in task), followed by a 1250 ms tracking phase and then a 500 ms posttrial fixation.

2.3 | Procedure

Participants were screened for normal or corrected-to-normal vision with a visual acuity letter chart. Bespoke Matlab programmes were used for trait inventories with mouse clicks to record responses on screen. The 74-item Schizotypal Personality Questionnaire (SPQ) (Raine, 1991) and 24-item, 5-point Subthreshold Autism Trait Questionnaire (SATQ) (Kanne et al., 2012) were used. The tracking task was separated into three blocks of gravity, inverted gravity and control. In the control condition, stimulus orientation was rotated by 90° from the gravity condition so that vertical motion was defined by Equations (1) and (2) and horizontal by (3) and (4) and gravity acted rightwards. Each block had 160 trials of 1.25 s duration with participant-initiated button presses to proceed (Figure 1b). Trials started with a 500 ms central dark grey fixation circle which disappeared at trial onset, and the stimulus was followed by a grey screen. Participants were instructed to fixate on the central spot and track the ball as well as they could. Blocks contained 80 fast and 80 slow trials and lasted approximately 10 min. The task interleaved the inventories with the conditions fixed in the same order, that is, SPQ, gravity, SATQ, inverted gravity and control, with breaks in between so that it lasted about 40 min. Key differences from the procedure of Meso et al. (2020) were that participants always started on the gravity condition, trials were shorter (1.25 s not 2 s), tasks included the control horizontal gravity condition, the ASD inventory was included and we used a higher precision psychophysics screen, the CRS Display++.

2.4 | Design and data analysis

We used a multivariate within-participants design. The independent variables were gravity direction with three levels: gravity (G)—downwards acceleration, acceleration against gravity (AG)—upwards and control (C)—rightwards and ball speed with two levels: slow (4°/s) and fast (16°/s). The key measures were the two inventories: the SPQ and SATQ, RMSE (root mean square unsigned error between dynamic eye position and ball position—and signed error for comparison) and saccades (rates and sizes). We also recorded participant age and sex. Data preprocessing to extract the RMSE and saccades used established methods. For saccade identifications, we used existing algorithms (Engbert & Kliegl, 2003) with slight modifications for sensitivity setting median speed threshold to $\lambda = 6$ and a longer restriction between saccade events of 30 ms with the rationale for these algorithm tweaks detailed in Meso et al. (2020). Before RMSE/signed error estimation, individual position traces were filtered with a fifth-order Butterworth filter with a cutoff at 50 Hz and velocity estimates obtained using

numerically differentiated position signals see (Meso et al., 2016; Meso et al., 2022). We reduced the RMSE responses to 25 samples, each covering a 20 ms window from onset at 0 to 500 ms (see examples inset in Figure 2). The viewed ball moved from the centre outwards and in the fast condition reached and bounced off the virtual vertical barriers depicted in dashed lines and example ball trajectory in Figure 1b. In this manipulation, all bounces happened after 500 ms and are not incorporated into the current analysis. The eye movements around the ball bounce represent another form of prediction to be studied in subsequent work. RMSE is a vector with separable horizontal and vertical components. It was computed for the *x*-direction capturing responses to the motion component at a *constant speed* for conditions G and AG (Figures 2 and 3, inset in light grey circles) and for the *y*-direction capturing responses subject to *acceleration due to simulated up/down gravity*.

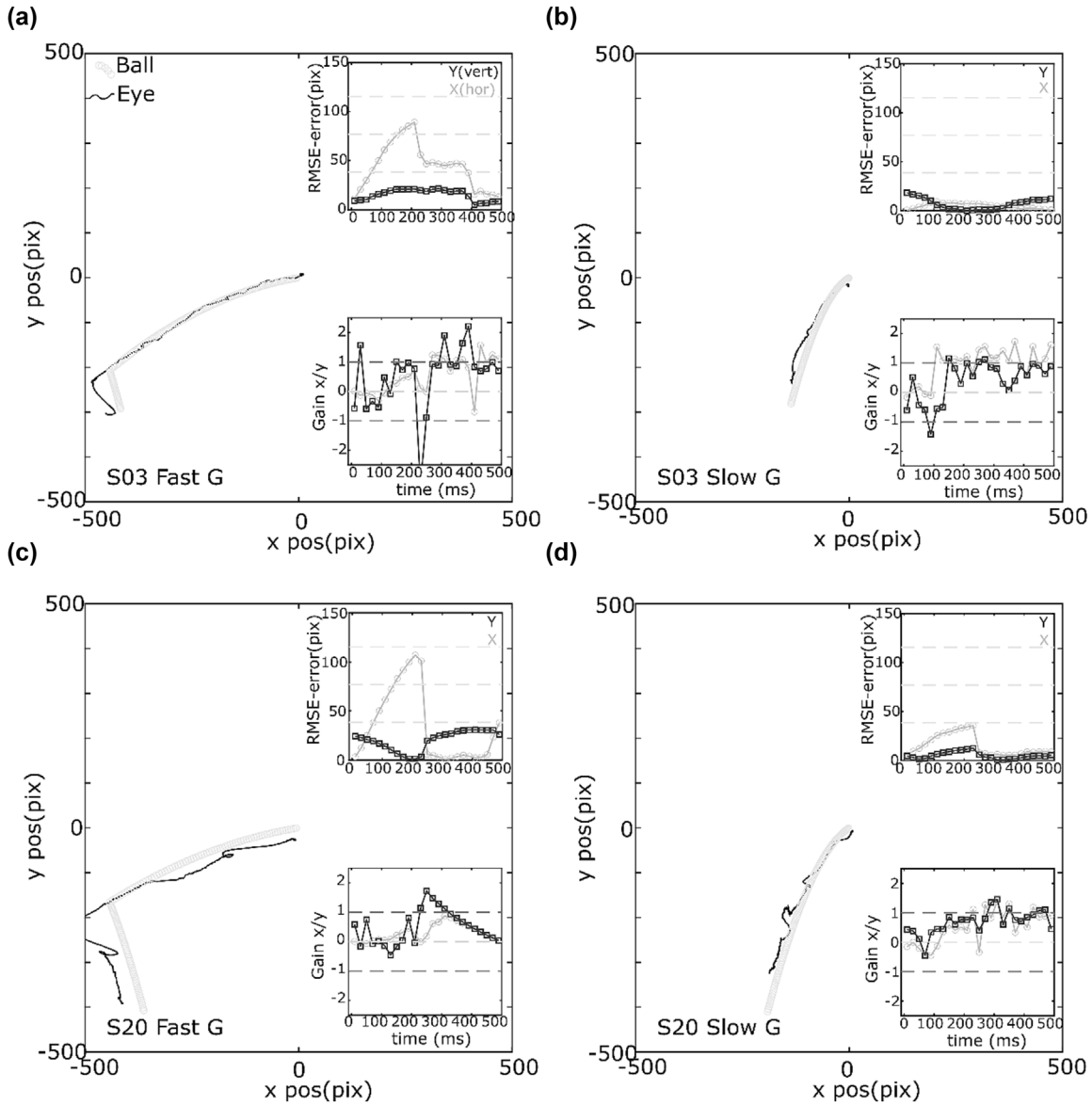

FIGURE 2 Example stimulus ball positions during trial (light grey unfilled circles) and corresponding raw unfiltered eye response (black line) in each main panel showing four selected representative trials for the downward gravity direction G. Insets in each main panel are two small panels with dynamic tracking unsigned position error, root mean square error (RMSE) for horizontal (grey circles) and vertical (black squares) directions on the top and for comparison dynamic speed based horizontal (grey circles) and vertical (black squares) gain estimates on the bottom. The two inset figures show data restricted to the 500 ms epoch which we analysed in the current work. Upper row data come from a better performing participant S03 under two conditions (a) fast gravity and (b) slow gravity. On the lower row are data from a second participant S20 with noisier responses under the conditions: (c) fast gravity and (d) slow gravity. Gain is generally more variable than RMSE as a performance measure and both measures approach optimal performance at 250–300 ms.

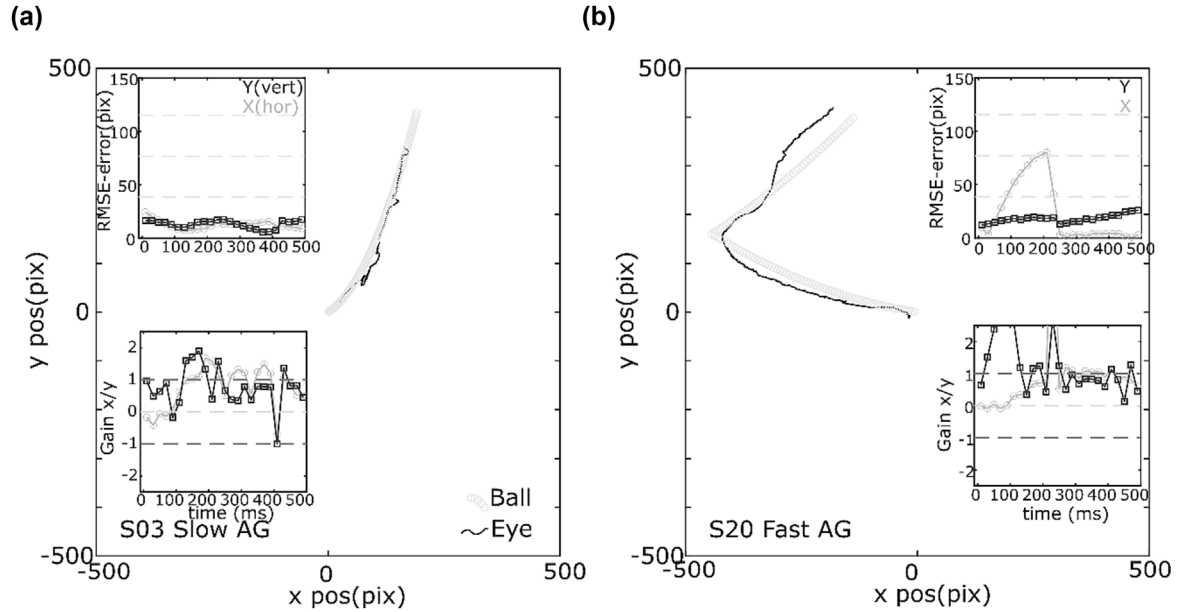

FIGURE 3 Example stimulus ball positions during the trial (grey unfilled circles) and eye response (black line), with similar structure to Figure 2 in each main panel with two selected representative trials from the condition in which acceleration was in the direction against gravity, AG. Insets in each main panel are two panels with unsigned root mean square error (RMSE) for horizontal (grey circles) and vertical (black squares) directions on the top and dynamic horizontal (grey circles) and vertical (black squares) speed gain estimates on the bottom. Participant S03 on the left shows better tracking than S20 on the right for the (a) slow and (b) fast conditions. In these examples, gain is much more variable over the 500 ms time-course of the trial considered than RMSE as a performance measure.

The examples of unsigned RMSE estimates from selected individual trials are shown alongside the classically used measure of gain in Figures 2 and 3 for the same condition with the latter based on position derivatives being more variable. We quantified learning as performance improvement during a block of 80 trials, by subtracting averaged RMSE value for the last 20 trials from that of the first 20 trials under the same speed condition. Learning was positive if there was improvement. We analysed the trait responses and a restricted subset of eye movement measures focusing on (i) the relationship between SPQ and SATQ, (ii) the relationship between the inventories and RMSE measures, (iii) the relationship between the inventories and the saccades and (iv) the dynamic changes in the relationships between both RMSE and saccades under the G and AG conditions. For each of the four, we ran correlations with alpha adjusted for the number of comparisons undertaken. (v) We also ran mean comparisons between gravity conditions for RMSE, Saccades and RMSE-learning. These were done using a Wilcoxon signed rank test because of the deviations from normality. Finally, we ran a correlation type PCA (Joliffe, 2002) to unpack the relationship between a restricted set of 21 measures. These variables were selected to cover subtraits of the SPQ and SATQ, saccade rates and amplitudes and RMSE measures, both at stimulus onset (0 ms) and during the open-loop of response (~160 ms). Meaningful components were identified using parallels analysis of the variance (Jolliffe & Cadima, 2016). For simplicity, instead of including all measures in the statistical analysis, we focused analysis on the slow speed condition which showed similar patterns to the faster condition but was an easier tracking task. Participants reported finding the slower cases easier and more comfortable to track.

3 | RESULTS

3.1 | Dynamic tracking performance across gravity conditions

We measured the dynamic RMSE value (difference between on-screen ball and eye position), a continuous measure which captures the accuracy of the tracking, every 20 ms over the first 500 ms, separately for horizontal and vertical components. In the horizontal direction, with ball motion at a constant speed (4 or 16°/s), average performance, RMSE-*x* gradually worsened between 0 and 200 ms. This was because horizontal speed and direction were unpredictable in each trial, and the stimulus-driven response, which typically starts after a latency of around 85–95 ms, required a catch-up saccade and so only improved after 200 ms (Figure 4a,e, darker grey traces).

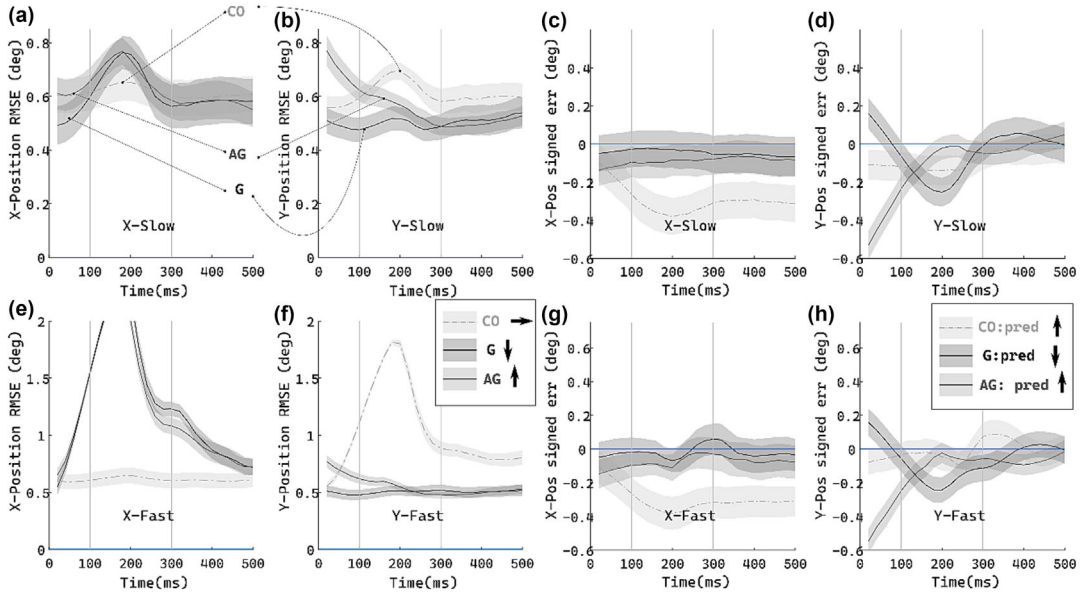

FIGURE 4 Dynamic root mean square error (RMSE) performance and signed error prediction measures in degrees plotted on the ordinate axis, mean and standard error for 48 participants, against time in ms from stimulus onset on the abscissa for gravity (black, G), inverted gravity (dark grey, AG) and control with horizontally accelerating gravity (light grey and dash/dot lines, CO) conditions. (a) RMSE for the horizontal direction in the slow condition. (b) Vertical direction RMSE, slow condition showing worse performance for AG from onset to 200 ms. (c) Signed error for the horizontal direction slow condition around zero for G/AG with the control (lightest grey) showing negative error under rightwards gravity. (d) Signed error for the vertical direction showing the darkest grey G trace cutting the *x*-axis reflecting prediction by the eye and the AG condition never crossing the *x*-axis but improving from onset. (e) Horizontal fast condition RMSE with catch-up saccades around 100-300 ms. (f) Vertical fast condition RMSE similar to (b) with better performance for G than AG. The control condition has gravity applied in the *x*-direction and is similar in dynamic trend to G condition but worse tracked by 0.1°. (g) Signed horizontal error for the fast condition similar to the slow condition (c). (h) Signed vertical error for the fast condition similar to (d) with the prediction direction key inset showing error direction that indicates the eye leads the ball.

For RMSE-*y* in the vertical direction where acceleration acted, the gravity condition was the same within each block of trials so motion could be predicted and anticipated by the participant after some trials. The average response is recorded as about 0.5° from onset for the full 500 ms (Figure 4b,f darkest grey trace). In contrast, for the inverted gravity condition, average tracking was worse at ∼0.8° from onset gradually improving until 300 ms, implying there was an anticipatory response in the direction of acceleration against gravity that was less effective than under gravity (Figure 4b,f mid grey trace). Note here that in a dynamic unsigned position error estimate, if the eye is static during the first 100 ms, then RMSE will typically get larger over time from onset as the ball moves away from the fixating eye, and we see this in most of the example single trial cases, inset in the light grey traces and circular markers in the *x*-direction of Figures 2 and 3. In contrast in the *y*-direction of the same panels, in the black square markers, we see that RMSE stay almost the same or reduce substantially over the first 100–200 ms. This result is consistent with the previous study (Meso et al., 2020), with worse performance and slower dynamics under AG. The differences are statistically evaluated in the next section. Importantly, the control condition with horizontal gravity was similar to the gravity condition but with a baseline averaged initial performance of 0.6°, 0.1° worse than the gravity condition (Figure 4a,e lightest grey trace). In these traces, gravity is applied in the *x*-direction for the control, and therefore, the like for like comparisons of G/AG and C is between the first and second columns of panels in Figure 4. This comparison suggests that there is a performance advantage for the downwards gravity condition that is reduced by 0.1° in the horizontal rightward gravity control condition. Unsigned RMSE measures performance in a task where participants are asked to track the target as closely as possible but does not capture whether the eye leads the ball or vice versa during tracking. To analyse that and estimate dynamic prediction, we similarly computed averaged signed error across all our participants and plot them in the same figure (Figure 4c,d,g,h). For signed error in the *x*-direction, for the first 500 ms for the G and AG conditions (overlapping darker greys in Figure 4c,g), traces overlap with the line through the *y* value of zero, and confidence intervals also overlap with zero, so the eye does not systematically lead or follow the

ball. For the vertical *y*-direction where stimulus acceleration is predictable, the key to the direction of a positive prediction which changes across conditions is shown in the inset in Figure 4H. For G, the eye trails the ball until a cross over point, which we calculate, on average, at 79 ms from onset after which the ball leads the eye until ~300 ms. In contrast, for AG, the eye trails the ball from onset getting slowly closer to it until about 200 ms when the signed error overlaps with the zero point (Figure 4d,h). Computing signed error 95% confidence intervals and analysing overlap with zero, we confirm that under G, signed error is positive at stimulus onset and becomes negative reflecting prediction, with the eye leading the ball downwards, around 150–250 ms for both the fast and slow conditions. For AG, however, signed error is below zero reflecting the ball leading the eye from onset until about 150 ms when confidence intervals start to overlap with zero. The corresponding control condition in the third column (Figure 4c,g) shows a different trend with errors getting worse from onset, but the ball leading the eye consistently. In summary, we see evidence for systematic prediction only under the G condition starting at 79 ms which is on average the stimulus-driven response threshold/latency, and in contrast a gradual anticipatory and stimulus-driven improvement of accuracy under AG, consistent with the RMSE results. We note that reports are based on the averages, but we see a diverse range of individual participant trends. We continue to use RMSE as our main dynamic performance measure based on our task instruction to track accurately.

3.2 | ASD and SPQ traits and links to eye tracking

The SPQ produced scores comparable with previous work with median = 16 and IQR = 18.5. Participant scores were almost evenly distributed below 30 (See Figure 5a). The SATQ produced scores comparable with previous work with median = 17.5 and IQR = 11.5, and scores were approximately normally distributed (Figure 5b). We ran a Pearson's correlation between the SPQ and SATQ and found a strong relationship between participant schizotypy and ASD trait levels with $r = 0.735$, $p = 2.73 \times 10^{-9}$(Figure 5c). At this initial analysis stage, we did not decompose the SPQ and SATQ into subclusters, to avoid expansion to the 15 possible permutations (3 SPQ clusters × 5 SATQ) and that decomposition was saved for subsequent analyses when we used PCA, a method more appropriate for data-driven multivariate analysis.

We then looked at the relationship between the inventories and the vertical RMSE-*y* at stimulus onset

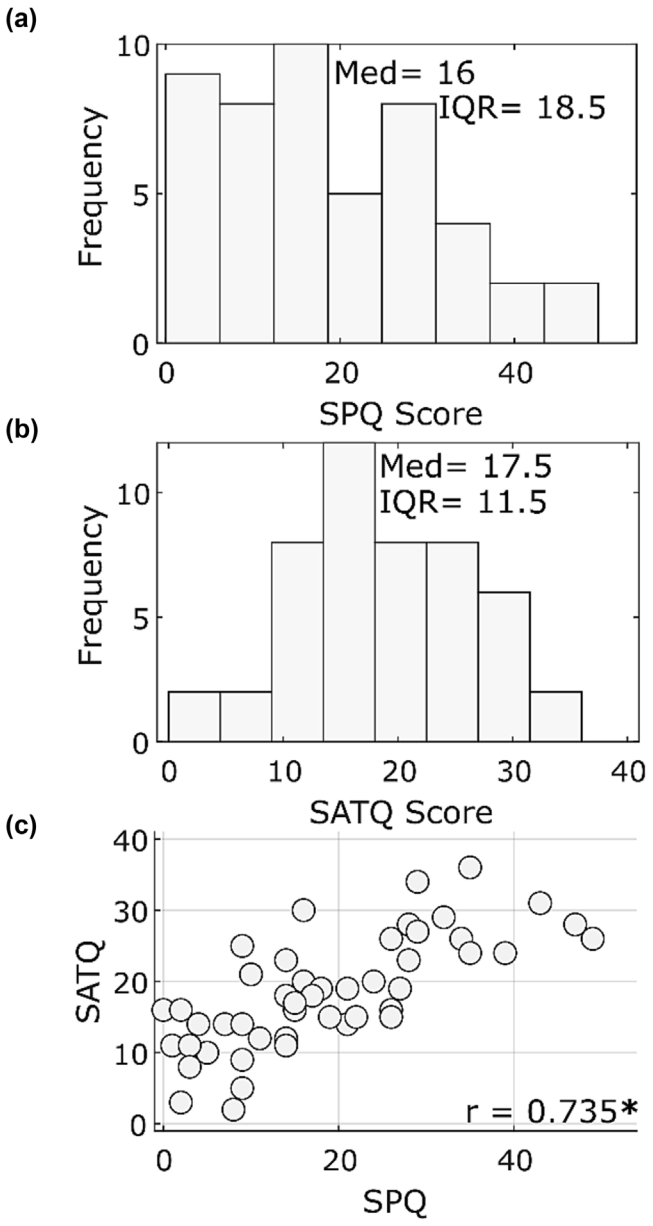

FIGURE 5 Summary of self-reported schizotypy (Schizotypal Personality Questionnaire [SPQ]) and autism spectrum disorder (Subthreshold Autism Trait Questionnaire [SATQ]) trait measures from 48 participants. Panels (a) and (b) show the frequency distributions of SPQ and SATQ scores with the median and interquartile range inset. (c) A strong correlation is found between SPQ and SATQ scores visualised in the scatter graph.

(0 ms), which reflects anticipatory responses. For the four comparisons using Pearson's correlation, we adjusted alpha for significance to 0.0125. Under the gravity condition, there was a near-zero correlation between the SPQ and RMSE-*y* with $r = -0.026$, $p = 0.86$ and similarly a low correlation between SATQ and RMSE-*y* at with $r = -0.074$, $p = 0.62$. Under the inverted gravity condition, there was a low correlation between the SPQ and the RMSE-*y* with $r = 0.065$, $p = 0.66$ and similarly

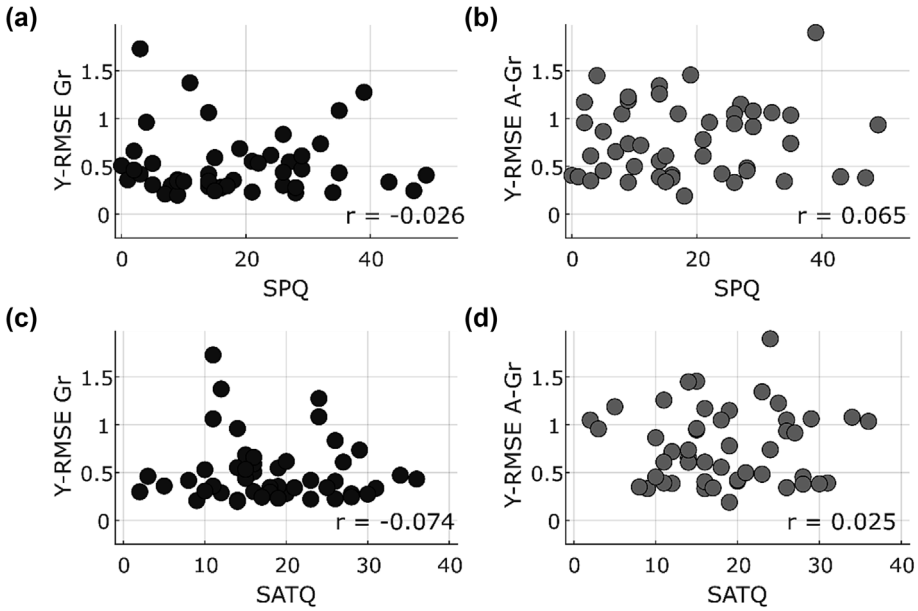

FIGURE 6 Participant data showing relationship between Schizotypal Personality Questionnaire (SPQ) (schizotypy) and Subthreshold Autism Trait Questionnaire (SATQ) (autism spectrum disorder [ASD]) inventory scores and root mean square error (RMSE) at stimulus onset. (a) Near-zero correlation between SPQ and RMSE for at 0 ms for gravity condition, G. (b) Weak correlation between SPQ and onset RMSE under inverted gravity, AG. (c) Weak correlation between SATQ and onset RMSE for G. (d) Near-zero correlation between SATQ and onset RMSE for AG.

between SATQ and RMSE-*y* with $r = 0.025$, $p = 0.86$. There was therefore no significant relationship between the trait measures and the tracking performance in the gravity direction at onset (Figure 6a–d).

We then analysed the relationship between the traits and the eight saccade measures, adjusting the alpha value for Pearson's correlations to 0.00625. Under the gravity condition, there was a nonsignificant negative correlation between the SPQ and the saccade rate, $r = -0.169$, $p = 0.25$, and similarly for the SATQ and saccade rate, $r = -0.153$, $p = 0.30$. Under the inverted gravity condition, the correlation was near zero for the SPQ and the saccade rates, $r = -0.047$, p = 0.75, and the SATQ and the saccade rate, $r = -0.039$, p = 0.79. The traits showed little relation to the rates (Figure 7a–d). For the saccade amplitudes, under the gravity condition, there was a nonsignificant negative correlation between the SPQ and the amplitudes, $r = -0.12$, $p = 0.40$, and the SATQ and amplitudes, $r = -0.12$, $p = 0.41$. For the inverted gravity condition, these were again near zero for SPQ and amplitude, $r = 0.041$, $p = 0.78$, and SATQ and amplitude, $r = -0.017$, $p = 0.91$. Traits therefore showed little obvious relationship with the amplitudes (Figure 7e–h).

3.3 | Onset, latency, open-loop and closed-loop RMSE across gravity conditions

Tracking was measured separately across G and AG conditions both for the constant speed component—*x* and the accelerating component—*y*. We first considered the relationship between the tracking measures for the accelerating direction RMSE-*y* for the G and AG conditions. We carried out four Pearson's correlations to track this relationship dynamically from onset (0 ms) through to the closed-loop response at 240 ms in four windows. Alpha was adjusted to 0.0125 for the four comparisons. There was a significant correlation between individual RMSE-*y* values across all the time windows: at 0 ms, $r = 0.422$, $p = 0.00282$; near response onset at 80 ms $r = 0.472$, $p = 7 \times 10^{-4}$; during the open-loop at 160 ms $r = 0.481$, $p = 5.47 \times 10^{-4}$; and during the closed-loop $r = 0.532$, $p = 9.8 \times 10^{-5}$. Interestingly, the correlations increase in strength over time from onset, suggesting that the earliest anticipatory responses have less shared processing between the G and AG stimulus cases than the later closed-loop response (Figure 8a–d). We then tested for a difference in the RMSE-*y* responses between the G and AG conditions for the same sequential time windows. We used a Wilcoxon signed rank test because of the nonparametric distributions (see Figure 8e–h). There was a significant difference between the G and AG responses for the earliest two windows, with the values at 0 ms for G: median = 0.41° and for AG: median = 0.73°, with $W = 167$, $p = 0.0000157$, and at 80 ms for G: median = 0.37° and for AG: median = 0.56°, with $W = 265$, $p = 0.000923$. At 160 and 240 ms, there was no significant difference between G and AG responses, with $W = 513$, $p = 0.44$ and $W = 550$, $p = 0.70$, respectively. Early responses in the gravity direction are consistently best for the G condition and initially poorer for the AG condition (Figure 8e–h; see also Figure 4). Similar differences are found between the G and control conditions (see Figure 4). The pattern of results showing better performance under G and delays under AG replicates previous findings (Meso et al., 2020).

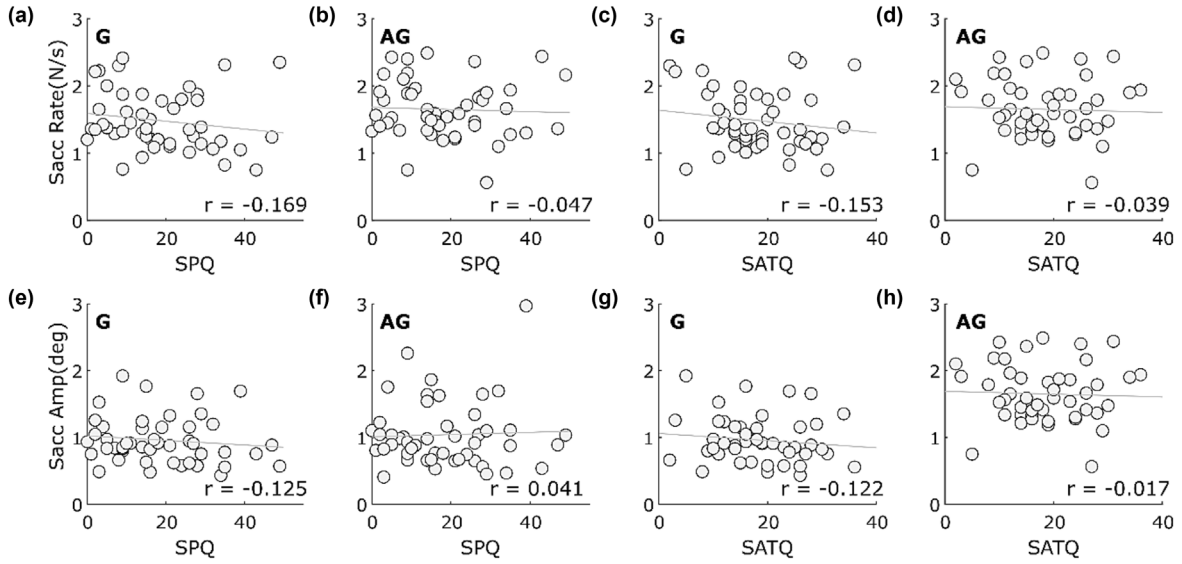

FIGURE 7 Relationship between schizotypy and autism spectrum disorder (ASD) trait measures and saccade metrics. Eye movements shown for the slow condition only. Panels (a) to (d) show weak negative correlation between both Schizotypal Personality Questionnaire (SPQ)/Subthreshold Autism Trait Questionnaire (SATQ) and saccade rates under both gravity and inverted gravity conditions; those for gravity in (a) and (c) have higher Pearson's correlation values than for inverted gravity by about 0.12. Panels (e) to (h) show weak to near zero correlations between SPQ/SATQ and saccade sizes/amplitudes for both gravity and inverted gravity.

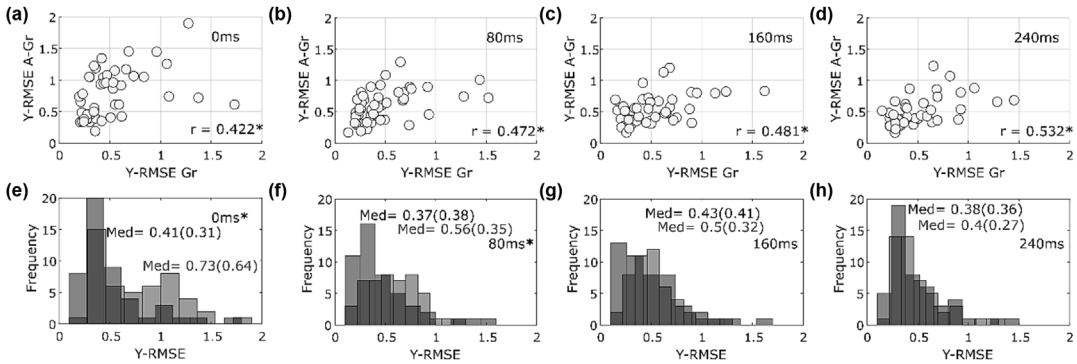

FIGURE 8 Root mean square error (RMSE) responses from all participants over four temporal windows from stimulus onset to the closed-loop compared between G and AG conditions. The correlation between RMSE values under gravity and inverted gravity shown in scatter graphs from (a) onset at 0 ms, (b) stimulus response latency at 80 ms, (c) within the open-loop at 160 ms and (d) during the closed-loop at 240 ms. The responses are correlated with significance indicated by (*), and the strength of correlation increases consistently from onset to the closed-loop, left to right in the panels. The RMSE values have nonparametric distributions that are visually compared across the same time windows (e) from onset, (f) through response latency, (g) the open-loop response and (h) the closed-loop. The asterisks at onset and response latency indicate a significant difference in nonparametric tests (see text for details) which is not maintained in the later windows. G is in black and AG in grey in the histograms.

3.4 | Other notable differences between gravity and inverted gravity conditions

We compared the values of both saccade measures under the two gravity conditions, adjusting alpha for the two Wilcoxon signed rank tests. For the rates, significantly fewer saccades are produced per second under G: median = 1.36 than under AG: median = 1.58, $W = 245$, $p = 0.000735$. For the amplitudes, there is no significant difference in the size of saccades produced under the G and AG conditions, $W = 448$, $p = 0.15$ (Figure 9a,b). Finally, we looked at the effect of learning across trials for both the constant speed motion with RMSE-x and the motion subject to acceleration RMSE-y and adjusted alpha for two comparisons to 0.025. For the first (x), there is a small significant difference between the conditions

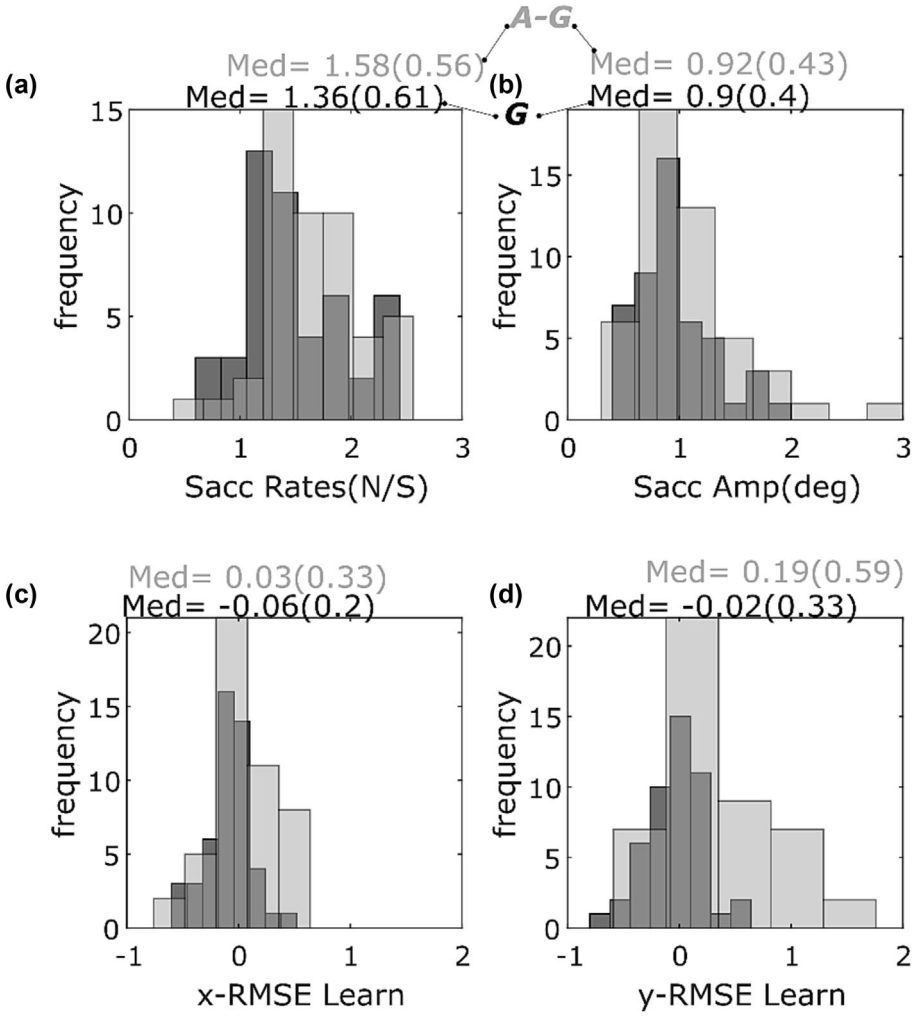

FIGURE 9 Differences between G (in darker grey) and AG (lighter grey) participant eye responses for key saccade metrics and learning estimated from root mean square error (RMSE), that is, tracking performance improvement during task. (a) Saccade rates are found to be different across gravity conditions in nonparametric tests (see text for details) with participants producing significantly more saccades per second under the G condition than AG. (b) There is little difference between the average size of saccades when G and AG are compared statistically. Learning over the blocks is estimated separately at trial onset for (c) horizontal direction showing little difference between G and AG, and (d) for the vertical direction, there is more learning for AG than G with a median of RMSE $= 0.19°$ and $-0.02°$ respectively. This suggests that G performance is good right from the early trials while AG improves during the block.

with less learning or improvement over the course of trials, under G: median $= -0.06°$ than AG: median $= 0.03°$, $W = 319$, $p = 0.0058$. For the accelerating condition (y), learning is again lower for G: median $= -0.02°$ than AG: median $= 0.19°$, $W = 248$, $p = 0.000488$. This result suggests that performance in the gravity condition which was better for all participants did not generally improve over the course of trials while that under the inverted gravity condition generally did, especially under the vertically accelerated direction (Figure 9c,d).

3.5 | Principal component analysis

Given the number of variables measured, we could not answer all questions of interest using standard correlations and hypothesis-based statistical tests without an explosion of familywise error. Like others (Meso et al., 2020; Nenadić et al., 2021), we took a data-driven approach and identified variables of interest for a correlation-based PCA. We selected a set of 21 measures from over 200 possible alternatives in the multivariate experiment including the AGE, the three main clusters of the SPQ, the five subtraits of the SATQ and eye tracking with both saccade and RMSE measures for the G and AG condition. Table 1 contains the PCA results with the 21 variables listed and their loadings for the first seven components. These seven components in the table (in descending order of their strength) are selected based on parallels analysis restricting explained data variance to 75%. We use the data loadings to guide our qualitative description of each of the orthogonal components. The first component is dominated by *eye movement measures* with little contribution from AGE and the inventories. It likely captures individual differences in eye movements which make some participants better at eye-tracking tasks than others. The second component captures *general overlap* between the SPQ and the SATQ, unrelated to eye movements. The third component is dominated by the *positive cluster of the SPQ* and the *odd, face and rigidity* traits of the SATQ. In

TABLE 1 Principal component analysis results looking at the relationship between variables covering the inventories, saccade metrics and tracking performance in the form of RMSE.

		Component #						
		1	**2**	**3**	**4**	**5**	**6**	**7**
	Variance (%)	20.0	17.9	10.2	8.3	7.3	5.6	4.8
	Variable name							
	AGE	−0.02	−0.16	0.03	**−0.28**	**−0.39**	0.10	−0.17
(Qs)	SPQ—positive	−0.02	**0.38**	**−0.23**	−0.02	0.03	0.19	**−0.22**
	SPQ—negative	−0.11	**0.35**	0.11	**−0.20**	0.19	0.00	−0.07
	SPQ—disorganised	−0.10	**0.39**	−0.16	0.04	−0.14	0.17	−0.03
	SATQ—social int.	−0.08	**0.31**	0.06	**−0.30**	**0.28**	−0.13	**0.38**
	SATQ—odd	−0.05	**0.23**	**−0.31**	0.11	**−0.34**	0.19	**0.24**
	SATQ—read faces	−0.04	**0.35**	**0.24**	0.00	−0.08	−0.01	**0.44**
	SATQ—language	−0.16	**0.30**	0.02	0.11	0.01	−0.13	**−0.37**
	SATQ—rigidity	−0.07	**0.24**	**−0.23**	**−0.29**	−0.04	−0.03	**−0.43**
(G)	Saccades—amplitude	**0.33**	−0.02	0.00	−0.19	**0.29**	−0.06	0.00
	RMSE-*y* (0 ms)	**0.32**	0.07	−0.10	**0.21**	−0.08	**−0.37**	−0.17
	Saccades—rate (200 ms)	**−0.30**	−0.06	−0.14	**0.35**	**0.31**	−0.07	0.03
	RMSE-*x* (160 ms)	0.14	0.17	**0.52**	0.18	0.05	0.18	**−0.20**
	RMSE-*y* (160 ms)	**0.23**	0.17	−0.07	**0.43**	−0.04	**−0.36**	−0.09
	RMSE-*y*, learn (0 ms)	−0.09	−0.15	−0.15	0.01	**0.51**	**0.24**	**−0.21**
(AG)	Saccades—amplitude	**0.37**	0.05	−0.13	**−0.22**	**0.27**	0.14	0.00
	RMSE-*y* (0 ms)	**0.37**	0.11	**−0.20**	0.04	0.06	0.10	0.19
	Saccades—rate (200 ms)	**−0.34**	0.02	−0.17	**0.32**	**0.20**	0.09	0.14
	RMSE-*x* (160 ms)	0.15	0.12	**0.45**	**0.26**	0.03	**0.41**	−0.10
	RMSE-*y* (160 ms)	**0.34**	0.11	−0.17	0.12	0.09	−0.03	0.10
	RMSE-*y*, learn (0 ms)	0.18	−0.10	**−0.25**	0.14	−0.10	**0.53**	0.04

Note: The first seven components explaining 75% of the variance are included. Selected variable labels are given in the first column. Numbers represent variable loadings with higher loadings above |0.20| highlighted.

addition, this third component also includes eye movement during *open-loop constant tracking (160 ms)* and *anticipatory inverted gravity tracking* responses and learning. The fourth captured *negative SPQ* and *social interaction* and *rigidity of the SATQ*. For eye movements, this component included *saccade rates/amplitudes* and *open-loop and anticipatory tracking under the gravity* condition. The fifth captured *social interactions* and *odd clusters of the SATQ* and for eye movements, *saccade rates* and *learning under the gravity* condition. Both the fourth and fifth components had a substantial contribution from AGE, but we were unable to interpret why this might be the case. We also noted that we had a narrow spread of participant ages due to mostly sampling university students. The sixth and seventh components were difficult to characterise, with the former being predominantly driven by eye movements and the latter by traits.

4 | DISCUSSION

In this work, we studied the relationship between both ASD and schizotypy traits, recently demonstrated to have overlapping characteristics (Abu-Akel et al., 2018; Ford et al., 2018; Nenadić et al., 2021) and their association with cognition and behaviour probed through a gravity tracking task (Meso et al., 2020). Both ASD and schizophrenia have been found to disrupt ocular motor function (Barnes, 2008; Johnson et al., 2016), and questions remain about the commonality of the specific disruption. In light of recent hypotheses suggesting that schizophrenia and ASD may be caused by deficits in the brain's prediction mechanisms (Sinha et al., 2014; Sterzer et al., 2019), we tested the link between ASD and schizotypy using a tracking task in which physics-based motion prediction played a key role. In this context, the work involved a conceptual replication and extension of

research which introduced the gravity ball tracking task. We found that participants were much better at tracking under the familiar gravity condition than when acceleration direction was reversed in the inverted gravity condition (Meso et al., 2020). This tracking task was different from more widely used predictive sinusoidal tracking with blanking along the trajectory (Faiola et al., 2020), as there was a predictive element because participant performance could be improved by the application of knowledge about gravity (Delle Monache et al., 2015; Jörges & López-Moliner, 2017; McIntyre et al., 2001). In the current work, we similarly demonstrated an advantage for the downward gravity condition over others and unpack the multitude of results from the multivariate eye movement and inventory measures by answering three broad questions. We first interpret the findings in the context of replicating and extending Meso et al. (2020) with additional controls. Second, we unveil differences in tracking dynamics and discuss their implications. Finally, we characterise the multidimensional relationship between eye movements, ASD traits and schizotypy.

4.1 | Replication of the gravity advantage in tracking

Participants were asked to track a moving ball in repeated trials within blocks of separate gravity conditions. As such, within two or three trials from the start of the block, participants could expect that the vertical component in the gravity and upwards inverted gravity conditions would have the same acceleration over trials within the block. Under the gravity condition, all participants were good at tracking throughout the half-second duration from motion onset we analysed. Tracking was about 20% better than under the control horizontal acceleration condition, in which gravity acted in the rightward direction, suggesting that implicit knowledge of the physics-based expectations of gravity enhanced visual tracking (Delle Monache et al., 2015; Jörges & López-Moliner, 2019; McIntyre et al., 2001). This difference in the horizontal acceleration control condition showed that the laws of physics applied were based on experience specifically for the downward and not the orthogonal direction. The inverted gravity condition engendered much larger individual differences in responses and poorer tracking than the control suggesting it went against an encoded prior (Jörges & López-Moliner, 2017). Some participants were able to anticipate the accelerating response in the upward direction around motion onset before the visual system could plausibly produce a stimulus-driven response suggesting a learned anticipatory response (Kowler et al., 2019). Over the duration of the trial, most were able to improve to a point at which tracking performance was best and at a plateau matched across all conditions by about 300 ms from onset. Looking at the signed error to analyse prediction, we also explicitly showed that only the ecologically relevant downward gravity condition generated stimulus-driven eye responses which on average preceded the ball position following response latency and during the open-loop. In the current work, we sought to better understand these dynamic differences across conditions. Meso et al. (2020) used linear mixed models to control for random effects and identify a relationship between schizotypy trait levels and both RMSE and saccades which involved an interaction with gravity direction condition. Here, we have extended this previous work, aiming to better understand how the dynamic eye response depended on violations of the physics of gravity and trait characteristics.

4.2 | Schizotypy and ASD trait relationships

We used two established and quick-to-answer inventories: one for ASD—the SATQ (Kanne et al., 2012) and the other for schizotypy—the SPQ (Raine, 1991). Individual scores for the two inventories were highly correlated. Large recent studies have shown that the two conditions are related and suggested that individuals with a clinical ASD diagnosis were about 3.5 times more likely to receive a concurrent diagnosis of schizophrenia (Zheng et al., 2018). Similarly, overlaps have been identified in traits of both ASD and schizotypy in healthy undiagnosed participants across multiple cultures (Abu-Akel et al., 2018; Nenadić et al., 2021). The heterogeneity of ASD and schizotypy traits means that the overlap can also be separated into quite distinct clusters, for example, a first encompassing negative schizotypy and poor social communication (ASD), a second encompassing positive schizotypy and attention to detail (ASD) and a third with less specific overlap (Abu-Akel et al., 2018; Nenadić et al., 2021). Indeed, our two inventories decomposed the trait measures into three broad dimensions (from nine smaller ones) for schizotypy and five dimensions for ASD (Kanne et al., 2012; Raine, 1991). We expected some of these subtrait dimensions to be associated with the specific eye movement metrics. When we measured the correlation between both overall single trait levels and various eye movement measures, there were no significant relationships identified. In our previous work (Meso et al., 2020`), relationships between entire trait measures and specific eye movements were only identified using linear mixed models once several sources of variability were parcelled out in the analysis as random effects. The

correlations carried out in the current work did not control for potential sources of variability, and several of our behavioural measures were very specific in terms of the temporal epoch or the neural substrate that they tapped into and so small effects could have been lost to the variability within the general trait measures. Instead, this motivated the use of a data-driven approach to parcel out the variance into the various contributions in a statistically similar way to what was achieved by the linear mixed models in Meso et al. (2020), to observe more subtle relationships.

4.3 | Gravity direction performance and dynamics

The gravity condition was generally found to be better performed than the inverted gravity condition. When the saccades rates were compared, fewer saccades per second were measured under the gravity conditions than the inverted gravity conditions. The sizes of these saccades were not different. This was probably driven by more catch-up saccades in the poorly performed inverted gravity condition. More saccades imply less smooth tracking which would be expected for less predictable stimuli (Kowler et al., 2019). We separated the tracking measure of RMSE into four response epochs from anticipatory at onset, sensory response threshold, open-loop response and finally a closed-loop response. This was done to reduce the complexity of the continuous tracking responses and capture key ocular motor signatures that isolate anticipatory responses, in the absence of the stimulus. Sensorimotor processing is dynamic starting from bottom-up unelaborated sensory responses and building towards later responses which incorporate sensorimotor feedback loops (Masson & Perrinet, 2012; Meso et al., 2022). We first looked at the relationship between the RMSE in the vertical response for both the gravity and inverted gravity conditions across the time windows. All four showed a significant relationship between performance in the gravity conditions, with the relationship weakest in the anticipatory responses before the sensory response was visible and getting progressively stronger, with a peak in the closed-loop epoch. This finding suggests that the anticipatory response is at least partially driven by separate mechanisms in the gravity and inverted gravity condition, with downward gravity able to draw on prior knowledge about the physics rules in a fast, pre-attentive way (Jörges & López-Moliner, 2017; McIntyre et al., 2001). Further, in the inverted gravity condition, the RMSE responses themselves were also poorest for the anticipatory condition and subsequently less poor at the threshold of stimulus response in the second epoch considered. Although, in both these earlier windows, RMSE was significantly different from the gravity response. In the latter two windows, responses were not different across the gravity and inverted gravity conditions. Late in the closed-loop ocular motor response, integrative processes serving motion estimation incorporate visual feedback and therefore error signals (Goettker et al., 2019; Meso et al., 2022). By contrasting open-loop and closed-loop responses to the earlier epochs, we were able to separate motion perception deficits previously characterised (Barnes, 2008) from specifically early prediction deficits which appear to be compensated for within a few hundred milliseconds (Koychev et al., 2016). On top of that, in contrasting the gravity and inverted gravity conditions in the multivariate analysis that followed, we have prediction scenarios involving the overfamiliar case of downward gravity and the rule-contravening case of inverted gravity. Differences between these could unpack some seemingly contradicting results on tracking deficits in schizotypy which were measured by Koychev et al. (2016) but not by Meyhöfer et al. (2015) though the latter found differences in bold activation in sensory areas for schizotypy groups.

Early predictive mechanisms which would apply physics laws of motion when anticipating ball movement at onset could use predictive signals encoded in FEF (Faiola et al., 2020; Schröder et al., 2022) incorporating representations of gravity from the cerebellum (MacNeilage & Glasauer, 2018) and in synchrony with sensory motion areas like MT and MST (Ono, 2015; Ono & Mustari, 2012). We measured learning as improvement of tracking performance over the course of a block and found that learning improved more in the inverted gravity than gravity condition, with improvement almost two and a half times in the accelerating vertical direction when compared with the constant speed horizontal direction. Participants were therefore able to get slightly better over the course of the trials, particularly for the inverted gravity condition in anticipating the upwards direction acceleration. This learning could not, however, extend to a level to match performance under the established prior knowledge about the physics of gravity in the downward condition.

4.4 | Multidimensional patterns identified

We used PCA to unpack the relationships between the different variables in this experiment and link the trait measures to the eye movements. PCA has previously been used to study trait measures from healthy populations (Nenadić et al., 2021) and with eye-tracking metrics

(Meso et al., 2020). PCA was ideal in this scenario given the multiple dimensions of the inventories (Kanne et al., 2012; Raine, 1991) reflecting the heterogeneity of the constructs of interest—ASD trait and schizotypy. We used a simple correlation form of PCA and parallels analysis to restrict our components of interest to seven (Jolliffe & Cadima, 2016). The ordered components become progressively less strong and therefore less dominant in the explanation of the trends in the results. The first two of these components explaining 38% of the variance separately captured all-round eye movement performance at 20% and nonspecific overlap between all dimensions of both inventories at about 18%. Interestingly, the variance driving these dominant components may explain why direct correlations between individual eye movement measures and the total inventory scores did not find strong relationships. Instead, these substantial separated parts of the variance may account for the strong correlation between inventories, which has a nonspecific profile overlap previously proposed (Abu-Akel et al., 2018; Zheng et al., 2018).

The next two components together accounting for just under 20% of the variance were the most interesting in the current work. These separated the negative schizotypy dimension from the positive dimension. In the first of these, the positive schizotypy was associated with the ASD trait dimensions of oddness and rigidity and related with opposite sign to the ability to read faces. This relationship is consistent with that identified by Nenadić et al. (2021). This component was also linked to tracking performance in the constant speed horizontal direction during the stimulus response, that is, a tracking eye movement that is more general and not dependent on prediction. In the vertical direction, however, the association was with the inverted gravity condition in the anticipatory response and inverted gravity learning metrics. Therefore, these eye movements suggest for the first time that this *positive-odd* cluster of traits may relate to general motion tracking while also associated with an ability to adapt to motion that contravenes expectations of the physics of gravity. This finding extends that of Meso et al. (2020), as well as previous work using blanking paradigms (Koychev et al., 2016).

The second of these components links the negative dimension of schizotypy with the ASD trait dimensions of social interaction and rigidity, consistent with previous work (Ford et al., 2018; Nenadić et al., 2021). This *negative-social* component is also strongly associated with tracking in the gravity direction, specifically under the gravity condition, both in the anticipatory and the later open-loop response. This result is therefore consistent with the possibility that participants' use of long-term learned prior information about gravity could be associated specifically with this negative-social dimension. Indeed, it has been hypothesised that schizophrenia and ASD are driven by poor predictive mechanisms that should be based on learned rules (Millard et al., 2022; Sinha et al., 2014; Sterzer et al., 2019), and gravity could represent such a prior (Jörges & López-Moliner, 2017; McIntyre et al., 2001; Meso et al., 2020).

Each of the three remaining components contributing just under 18% of the total variance was less reliably interpretable, because of potentially spurious high age-related correlation, nonspecific associations with either eye movements or equally nonspecific relationships between inventory responses. The key finding in the current work is therefore in the characteristic eye movements associated with the *positive-odd* and *negative-social* trait dimensions. Interestingly, in both cases, there is an association with predictive tracking. In the case of *negative-social*, this is the application of physics rules associated with gravity. In the case of *positive-odd*, the predictive rule applied is a direct contravention to the hard-wired physics laws and so there is higher variability in predictive success. Based on the work of Faiola et al. (2020) identifying a key predictive role for FEF and connected areas and other work implicating the cerebellum in learning and encoding gravity (Mackrous et al., 2019; MacNeilage & Glasauer, 2018), we can make a testable prediction that downward gravity stimuli would specifically drive stronger predictive responses in both the FEF and the cerebellum. On the other hand, the *positive-odd* case is associated with the learning of physics rules that enable prediction but contravene expectations of natural physics. In such a context, we expect that there will still be contributions from the FEF to support the anticipatory aspects of the task particularly in individuals who learn the novel acceleration condition, but we expect less of a contribution from the cerebellum in terms of physics rules of gravity (Dakin et al., 2018; MacNeilage & Glasauer, 2018). There may also be additional compensatory responses from the supplementary eye fields, dorsal lateral pre-frontal cortex and sensory motion areas (Masson & Perrinet, 2012; Meyhöfer et al., 2015; Johnson et al., 2016) which come in during the sensory response and open-loop period to improve tracking performance.

4.5 | Conclusion

In this work, we showed that the participant tracking of the motion of a ball subjected to downward gravity was faster and better than tracking under the contravention of physics rules introduced by our inverted gravity condition. Performance, however, revealed large individual differences which we analysed along with inventories of

ASD traits and schizotypy, to unveil two key findings which come with testable predictions. The first is that the positive-odd cluster of characteristics is expected to be specifically associated with the use of learnt rules that contravene physics, while the second is that the *negative-social* cluster is expected to be associated with the exploitation of an established potentially pre-attentive prior of the physics laws of motion under gravity. We therefore encourage colleagues to consider testing these arising predictions in imaging, behavioural and clinical studies.

AUTHOR CONTRIBUTIONS

Chloe Cooper: Data curation; formal analysis; investigation; methodology; project administration; resources; software; validation; visualization; writing—original draft; writing—review and editing. **Andrew Isaac Meso:** Conceptualization; data curation; formal analysis; investigation; methodology; project administration; resources; software; supervision; validation; visualization; writing—original draft; writing—review and editing.

ACKNOWLEDGEMENTS

We thank Bournemouth University for financial support during the experiments and King's College London for subsequent financial support. We also thank colleagues at the Institute de Neuroscience de la Timone in Marseille for useful discussions during the preparation of the manuscripts. Finally, we thank the anonymous reviewers for helpful suggestions made.

CONFLICT OF INTEREST STATEMENT

The authors declare no conflicts of interest.

PEER REVIEW

The peer review history for this article is available at https://www.webofscience.com/api/gateway/wos/peer-review/10.1111/ejn.16169.

DATA AVAILABILITY STATEMENT

We will make data fully available following any requests and encourage further analyses of the datasets. Following publication, we will make anonymised data available online.

ORCID

Andrew Isaac Meso https://orcid.org/0000-0002-1919-7726

REFERENCES

Abu-Akel, A., Testa, R. R., Jones, H. P., Ross, N., Skafidas, E., Tonge, B., & Pantelis, C. (2018). Attentional set-shifting and social abilities in children with schizotypal and comorbid autism spectrum disorders. *The Australian and New Zealand Journal of Psychiatry*, *52*(1), 68–77. https://doi.org/10.1177/0004867417708610

Barnes, G. R. (2008). Cognitive processes involved in smooth pursuit eye movements. *Brain and Cognition*, *68*(3), 309–326. https://doi.org/10.1016/j.bandc.2008.08.020

Barrantes-Vidal, N., Gross, G. M., Sheinbaum, T., Mitjavila, M., Ballespi, S., & Kwapil, T. R. (2013). Positive and negative schizotypy are associated with prodromal and schizophrenia-spectrum symptoms. *Schizophrenia Research*, *145*(1–3), 50–55. https://doi.org/10.1016/j.schres.2013.01.007

Brainard, D. H., & Vision, S. (1997). The psychophysics toolbox. *Spatial Vision*, *10*(4), 433–436. https://doi.org/10.1163/156856897X00357

Chisholm, K., Lin, A., Abu-Akel, A., & Wood, S. J. (2015). The association between autism and schizophrenia spectrum disorders: A review of eight alternate models of co-occurrence. *Neuroscience & Biobehavioral Reviews*, *55*, 173–183. https://doi.org/10.1016/j.neubiorev.2015.04.012

Churchland, A. K., & Lisberger, S. G. (2002). Gain control in human smooth-pursuit eye movements. *Journal of Neurophysiology*, *87*(6), 2936–2945. https://doi.org/10.1152/jn.2002.87.6.2936

Dakin, C. J., Peters, A., Giunti, P., & Day, B. L. (2018). Cerebellar degeneration increases visual influence on dynamic estimates of verticality. *Current Biology*, *28*(22), 3589–3598. https://doi.org/10.1016/j.cub.2018.09.049

De Giorgi, R., de Crescenzo, F., D'Alò, G. L., Rizzo Pesci, N., di Franco, V., Sandini, C., & Armando, M. (2019). Prevalence of non-affective psychoses in individuals with autism spectrum disorders: A systematic review. *Journal of Clinical Medicine*, *8*(9), 1304. https://doi.org/10.3390/jcm8091304

Delle Monache, S., Lacquaniti, F., & Bosco, G. (2015). Eye movements and manual interception of ballistic trajectories: Effects of law of motion perturbations and occlusions. *Experimental Brain Research*, *233*(2), 359–374. https://doi.org/10.1007/s00221-014-4120-9

Engbert, R., & Kliegl, R. (2003). Microsaccades uncover the orientation of covert attention. *Vision Research*, *43*(9), 1035–1045. https://doi.org/10.1016/S0042-6989(03)00084-1

Faiola, E., Meyhöfer, I., & Ettinger, U. (2020). Mechanisms of smooth pursuit eye movements in schizotypy. *Cortex*, *125*, 190–202. https://doi.org/10.1016/j.cortex.2019.12.008

Ford, T. C., Apputhurai, P., Meyer, D., & Crewther, D. P. (2018). Cluster analysis reveals subclinical subgroups with shared autistic and schizotypal traits. *Psychiatry Research*, *265*, 111–117. https://doi.org/10.1016/j.psychres.2018.04.037

Goettker, A., Braun, D. I., & Gegenfurtner, K. R. (2019). Dynamic combination of position and motion information when tracking moving targets. *Journal of Vision*, *19*(7), 2–2. https://doi.org/10.1167/19.7.2

Goettker, A., & Gegenfurtner, K. R. (2021). A change in perspective: The interaction of saccadic and pursuit eye movements in oculomotor control and perception. *Vision Research*, *188*, 283–296. https://doi.org/10.1016/j.visres.2021.08.004

Johnson, B. P., Lum, J. A., Rinehart, N. J., & Fielding, J. (2016). Ocular motor disturbances in autism spectrum disorders: Systematic review and comprehensive meta-analysis. *Neuroscience*

and Biobehavioral Reviews, *69*, 260–279. https://doi.org/10.1016/j.neubiorev.2016.08.007

Jolliffe, I. T. (2002). *Principal component analysis* (2nd ed.). Springer.

Jolliffe, I. T., & Cadima, J. (2016). Principal component analysis: A review and recent developments. *Philosophical Transactions. Series A, Mathematical, Physical, and Engineering Sciences*, *374*(2065), 20150202. https://doi.org/10.1098/rsta.2015.0202

Jörges, B., Hagenfeld, L., & López-Moliner, J. (2018). The use of visual cues in gravity judgements on parabolic motion. *Vision Research*, *149*, 47–58. https://doi.org/10.1016/j.visres.2018.06.002

Jörges, B., & López-Moliner, J. (2017). Gravity as a strong prior: Implications for perception and action. *Frontiers in Human Neuroscience*, *11*, 203. https://doi.org/10.3389/fnhum.2017.00203

Jörges, B., & López-Moliner, J. (2019). Earth gravity-congruent motion benefits pursuit gain for parabolic trajectories. *Journal of Vision*, *19*(10), 302b–302b.

Kanne, S. M., Wang, J., & Christ, S. E. (2012). The subthreshold autism trait questionnaire (SATQ): Development of a brief self-report measure of subthreshold autism traits. *Journal of Autism and Developmental Disorders*, *42*(5), 769–780. https://doi.org/10.1007/s10803-011-1308-8

Klopper, F., Testa, R., Pantelis, C., & Skafidas, E. (2017). A cluster analysis exploration of autism spectrum disorder subgroups in children without intellectual disability. *Research in Autism Spectrum Disorders*, *36*, 66-78. https://doi.org/10.1016/j.rasd.2017.01.006

Kowler, E., Rubinstein, J. F., Santos, E. M., & Wang, J. (2019). Predictive smooth pursuit eye movements. *Annual Review of Vision Science*, *5*, 223–246. https://doi.org/10.1146/annurev-vision-091718-014901

Koychev, I., Joyce, D., Barkus, E., Ettinger, U., Schmechtig, A., Dourish, C. T., Dawson, G. R., Craig, K. J., & Deakin, J. F. W. (2016). Cognitive and oculomotor performance in subjects with low and high schizotypy: Implications for translational drug development studies. *Translational Psychiatry*, *6*(5), e811. https://doi.org/10.1038/tp.2016.64

Mackrous, I., Carriot, J., Jamali, M., & Cullen, K. E. (2019). Cerebellar prediction of the dynamic sensory consequences of gravity. *Current Biology*, *29*(16), 2698, e2694–2710. https://doi.org/10.1016/j.cub.2019.07.006

MacNeilage, P. R., & Glasauer, S. (2018). Gravity perception: The role of the cerebellum. *Current Biology*, *28*(22), R1296–R1298. https://doi.org/10.1016/j.cub.2018.09.053

Masson, G. S., & Perrinet, L. U. (2012). The behavioral receptive field underlying motion integration for primate tracking eye movements. *Neuroscience and Biobehavioral Reviews*, *36*(1), 1–25. https://doi.org/10.1016/j.neubiorev.2011.03.009

McIntyre, J., Zago, M., Berthoz, A., & Lacquaniti, F. (2001). Does the brain model Newton's laws? *Nature Neuroscience*, *4*(7), 693–694. https://doi.org/10.1038/89477

Meso, A. I., De Vai, R. L., Mahabeer, A., & Hills, P. J. (2020). Evidence of inverted gravity-driven variation in predictive sensorimotor function. *European Journal of Neuroscience*, *52*(12), 4803–4823. https://doi.org/10.1111/ejn.14926

Meso, A. I., Gekas, N., Mamassian, P., & Masson, G. S. (2022). Speed estimation for visual tracking emerges dynamically from nonlinear frequency interactions. *Eneuro*, *9*(3), 0511-21. https://doi.org/10.1523/ENEURO.0511-21.2022

Meso, A. I., Montagnini, A., Bell, J., & Masson, G. S. (2016). Looking for symmetry: Fixational eye movements are biased by image mirror symmetry. *Journal of Neurophysiology*, *116*(3), 1250–1260. https://doi.org/10.1152/jn.01152.2015

Meso, A. I., Rankin, J., Faugeras, O., Kornprobst, P., & Masson, G. S. (2016). The relative contribution of noise and adaptation to competition during tri-stable motion perception. *Journal of Vision*, *16*(15), 6. https://doi.org/10.1167/16.15.6

Meyhöfer, I., Steffens, M., Kasparbauer, A., Grant, P., Weber, B., & Ettinger, U. (2015). Neural mechanisms of smooth pursuit eye movements in schizotypy. *Human Brain Mapping*, *36*(1), 340–353. https://doi.org/10.1002/hbm.22632

Millard, S. J., Bearden, C. E., Karlsgodt, K. H., & Sharpe, M. J. (2022). The prediction-error hypothesis of schizophrenia: New data point to circuit-specific changes in dopamine activity. *Neuropsychopharmacology*, *47*(3), 628–640. https://doi.org/10.1038/s41386-021-01188-y

Nelson, M. T., Seal, M. L., Pantelis, C., & Phillips, L. J. (2013). Evidence of a dimensional relationship between schizotypy and schizophrenia: A systematic review. *Neuroscience & Biobehavioral Reviews*, *37*(3), 317–327. https://doi.org/10.1016/j.neubiorev.2013.01.004

Nenadić, I., Meller, T., Evermann, U., Schmitt, S., Pfarr, J. K., Abu-Akel, A., & Grezellschak, S. (2021). Subclinical schizotypal vs. autistic traits show overlapping and diametrically opposed facets in a non-clinical population. *Schizophrenia Research*, *231*, 32–41. https://doi.org/10.1016/j.schres.2021.02.018

Ono, S. (2015). The neuronal basis of on-line visual control in smooth pursuit eye movements. *Vision Research*, *110*, 257–264. https://doi.org/10.1016/j.visres.2014.06.008

Ono, S., & Mustari, M. J. (2012). Role of MSTd extraretinal signals in smooth pursuit adaptation. *Cerebral Cortex*, *22*(5), 1139–1147. https://doi.org/10.1093/cercor/bhr188

Pelli, D. G. (1997). The VideoToolbox software for visual psychophysics: Transforming numbers into movies. *Spatial Vision*, *10*(4), 437–442. https://doi.org/10.1163/156856897X00366

Raine, A. (1991). The SPQ—A scale for the assessment of schizotypal personality based on DSM-III-R criteria. *Schizophrenia Bulletin*, *17*(4), 555–564. https://doi.org/10.1093/schbul/17.4.555

Schröder, R., Baumert, P. M., & Ettinger, U. (2021). Replicability and reliability of the background and target velocity effects in smooth pursuit eye movements. *Acta Psychologica*, *219*, 103364. https://doi.org/10.1016/j.actpsy.2021.103364

Schröder, R., Faiola, E., Fernanda Urquijo, M., Bey, K., Meyhöfer, I., Steffens, M., Kasparbauer, A. M., Ruef, A., Högenauer, H., Hurlemann, R., Kambeitz, J., Philipsen, A., Wagner, M., Koutsouleris, N., & Ettinger, U. (2022). Neural correlates of smooth pursuit eye movements in schizotypy and recent onset psychosis: A multivariate pattern classification approach. *Schizophrenia Bulletin Open*, *3*(1), sgac034. https://doi.org/10.1093/schizbullopen/sgac034

Sinha, P., Kjelgaard, M. M., Gandhi, T. K., Tsourides, K., Cardinaux, A. L., Pantazis, D., Diamond, S. P., & Held, R. M.

(2014). Autism as a disorder of prediction. *PNAS*, *111*(42), 15220–15225. https://doi.org/10.1073/pnas.1416797111

Sterzer, P., Voss, M., Schlagenhauf, F., & Heinz, A. (2019). Decision-making in schizophrenia: A predictive-coding perspective. *NeuroImage*, *190*, 133–143. https://doi.org/10.1016/j.neuroimage.2018.05.074

Zheng, Z., Zheng, P., & Zou, X. (2018). Association between schizophrenia and autism spectrum disorder: A systematic review and meta-analysis. *Autism Research*, *11*(8), 1110–1119. https://doi.org/10.1002/aur.1977

How to cite this article: Cooper, C., & Meso, A. I. (2023). Cognitive-perceptual traits associated with autism and schizotypy influence use of physics during predictive visual tracking. *European Journal of Neuroscience*, *58*(10), 4236–4254. https://doi.org/10.1111/ejn.16169